Received: 16 October 2018 | Revised: 21 December 2018 | Accepted: 4 January 2019

DOI: 10.1002/psc.3148

RESEARCH ARTICLE

WILEY Journal of PeptideScience

Synthesis of peptides containing oxo amino acids and their crystallographic analysis

Mrinal Kalita[1] | Archana Archana[2] | Astha Dimri[2] | Prema G. Vasudev[2] | Ramesh Ramapanicker[1]

[1] Department of Chemistry, Indian Institute of Technology Kanpur, Kanpur, India

[2] Metabolic and Structural Biology Division, CSIR-Central Institute of Medicinal and Aromatic Plants, Lucknow, India

Correspondence
Ramesh Ramapanicker, Department of Chemistry, Indian Institute of Technology Kanpur, Kanpur, UP 208016, India.
Email: rameshr@iitk.ac.in

Prema G. Vasudev, Metabolic and Structural Biology Division, CSIR-Central Institute of Medicinal and Aromatic Plants, Lucknow, India.
Email: premavasudev@cimap.res.in

Funding information
Science and Engineering Research Board, Grant/Award Number: SB/S5/GC-07/2014

An isolated uncharged hydrogen bond acceptor such as the carbonyl functionality of an aldehyde or a keto group is absent in natural amino acids. Although glutamine and asparagine are known to hydrogen bond through the amide carbonyl group in their side chains, they also possess the amide $-NH_2$ group, which can act as a hydrogen bond donor. This makes the structural study of peptides containing an oxo residue, with an isolated carbonyl group in the side chain, interesting. Here, we report the synthesis of δ- and ε-oxo amino acids and their incorporation into oligopeptides as the N-terminal residue. The resultant oxo peptides were extensively studied using X-ray crystallography to understand the interactions offered by the oxo group in peptide crystals. We find that the oxo groups are capable of providing additional hydrogen bonding opportunities to the peptides, resulting in increased intermolecular interactions in crystals. The study thus offers avenues for the utilization of oxo residues to introduce intermolecular interactions in synthetic peptides.

KEYWORDS

hydrogen bonds, oligopeptides, oxo amino acids, side chain modification, X-ray diffraction

1 | INTRODUCTION

Peptides that self-assemble into predefined structures are increasingly being designed and studied as they find unparalleled applications in material and biomedical sciences.[1-9] Modification of peptides to improve intermolecular hydrogen bonding, hydrophobic, electrostatic, and aromatic interactions can augment their self-assembling properties.[10-13] Therefore, introduction of functional groups into the side chains of synthetic peptides that can increase the propensity to self-assemble is relevant and interesting. Isolated carbonyl (oxo) groups such as an aldehyde or a keto group are not found in proteinogenic amino acids as a side chain functionality. We assumed that if an oxo group is incorporated into the side chains of oligopeptides, it may lead to unprecedented intermolecular interactions through hydrogen bonding. Helical segments of proteins are known to stabilize their N-terminus through hydrogen bonding with the carbonyl oxygen of glutamine and asparagine.[14,15] However, the effect of an isolated oxo group is yet to be studied. This particular scenario prompted us to prepare oxo amino acids and incorporate them into peptides to examine the structural effects such a group can impart. Here, we report the synthesis of δ- and ε-oxo amino acids by extending a methodology that we had earlier reported for the synthesis of γ-aryl γ-oxo α-amino acids and the incorporation of these residues on the N-terminus of six oligopeptides. The N-terminal residues in peptides **1** to **5** have a δ-oxo group, and that in peptide **6** has a ε-oxo group (Figure 1). The amino acid sequences of the peptides were chosen to ensure a higher propensity to form helical structures in crystals. The crystal structures of these peptides were then studied in detail to understand the effect of oxo groups in crystal packing.

2 | RESULTS AND DISCUSSION

2.1 | Synthesis of oxo amino acids and oxopeptides

The oxo amino acids were synthesized following a procedure that we had developed for the synthesis of γ-aryl γ-oxo α-amino acids from 1,3-dithiane derivatives of aromatic aldehydes and an iodide derived

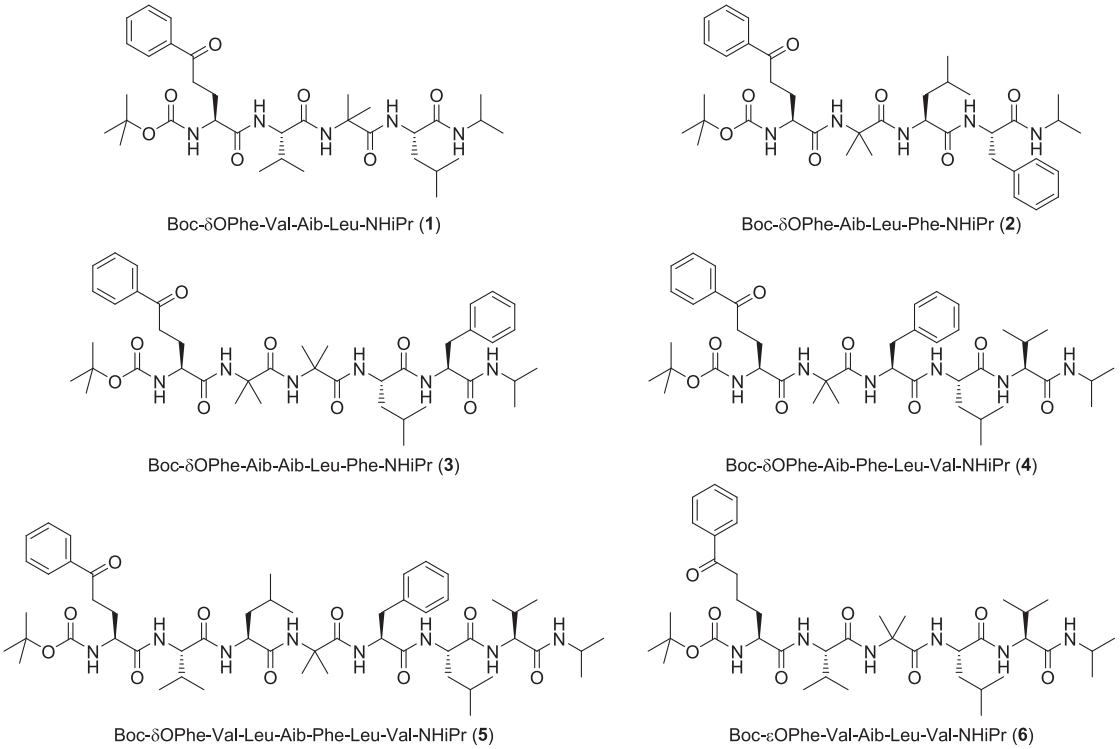

FIGURE 1 Oxo peptides **1** to **6**

from serine.[16] We assumed that a γ-oxo group would be too close to the peptide backbone and decided to base this study on δ- and ε-oxo amino acids. Accordingly, the two oxo amino acid derivatives **11a** and **11b** were prepared from the iodide derivatives **7a** and **7b**, respectively (Scheme 1). Iodides **7a** and **7b** were prepared from L-aspartic acid and L-glutamic acid, respectively, using reported procedures.[17] The iodides **7a** and **7b** were treated with 2-phenyl-1,3-dithiane in the presence of *n*-butyllithium (*n*-BuLi, −50 °C, tetrahydrofuran [THF]) to get the products **8a** and **8b**, respectively. The oxazolidine rings in **8** were hydrolyzed by treating with 7% trifluoroacetic acid (TFA) in methanol for 10 hours to get the *N*-Boc amino alcohol derivatives, **9a** and **9b**. Hydrolysis of **9a** and **9b** with I_2 and saturated $NaHCO_3$ solution (CH_3CN, 0 °C, 1 h) yielded the oxo amino alcohol derivatives **10a** and **10b**. The primary hydroxyl groups in **10a** and **10b** were oxidized to the corresponding carboxylic acid groups to get the required amino acid derivatives **11a** and **11b** in overall yields of 47% and 45% from **7a** and **7b**, respectively (Scheme 1).

Peptides **1** to **5** were prepared from the δ-oxo amino acid derivative **11a**, and peptide **6** was prepared from the ε-oxo amino acid derivative **11b**. Coupling **11a** with H-Val-Aib-Leu-NH^{i}Pr, H-Aib-Leu-Phe-NH^{i}Pr, H-Aib-Aib-Leu-Phe-NH^{i}Pr, H-Aib-Leu-Val-Phe-NH^{i}Pr, and H-Val-Leu-Aib-Phe-Leu-Val-NH^{i}Pr under standard solution-phase peptide coupling conditions (EDC·HCl, hydroxybenzotriazole [HOBt], CH_2Cl_2, 0 °C-room temperature [rt], 10 h) yielded oxo peptides **1** to

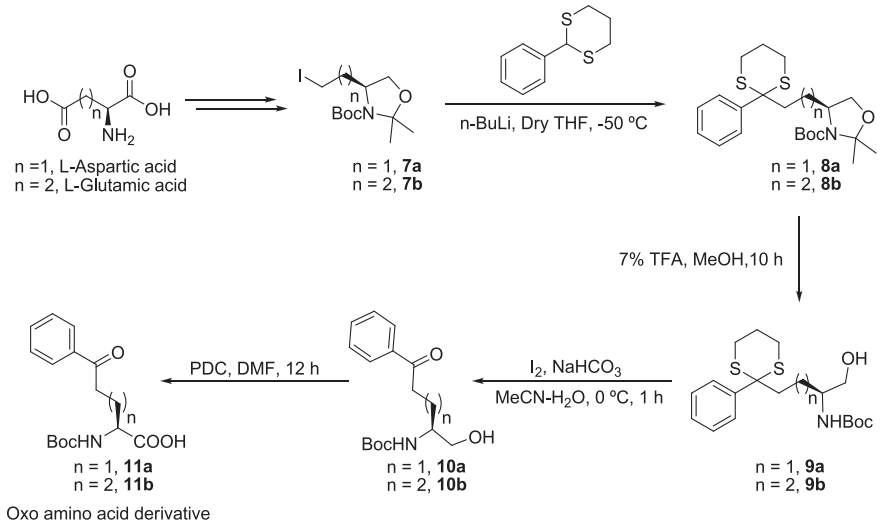

SCHEME 1 Synthesis of δ-oxo amino acid derivative **11a** and ε-oxo amino acid derivative **11b**. DMF, dimethylformamide; MeOH, methanol; n-BuLi, *n*-butyllithium; PDC, pyridinium dichromate; TFA, trifluoroacetic acid; THF, tetrahydrofuran

5. Similarly, coupling of **11b** with H-Val-Aib-Leu-Val-NH^{i}Pr under the same conditions as above yielded peptide **6**. Peptides **1** and **2** are tetrapeptides; **3**, **4**, and **6** are pentapeptides; and **5** is a heptapeptide.

2.2 | Crystallographic analysis of peptides 1 to 6

2.2.1 | Molecular conformations

Figure 2 shows the molecular conformations of peptides **1** to **6** in crystals. All the peptides adopted helical conformations as expected from the propensities of the constituent amino acids. Aib residues have been introduced into these peptides to facilitate helix nucleation and crystallization.[18-21] Backbone dihedral angles and hydrogen bonding parameters of all the structures are listed in Tables 1 and 2. Tetrapeptide **1**, heptapeptide **5**, and pentapeptide **6** adopt 3_{10}-helical conformations, with a transition to α-helical conformation at the C-terminus. Peptides **2** and **3** are 3_{10}-helices, stabilized by three and four consecutive 4 → 1 hydrogen bonds, respectively. Two polymorphic crystals of peptide **4** provide a total of three different molecular conformations of the peptide. One of the molecules (MOL-2) in polymorph **4a** is an α-helix with three consecutive 5 → 1 hydrogen bonds and an additional 4 → 1 hydrogen bond (N3···O0) at the N-terminus,

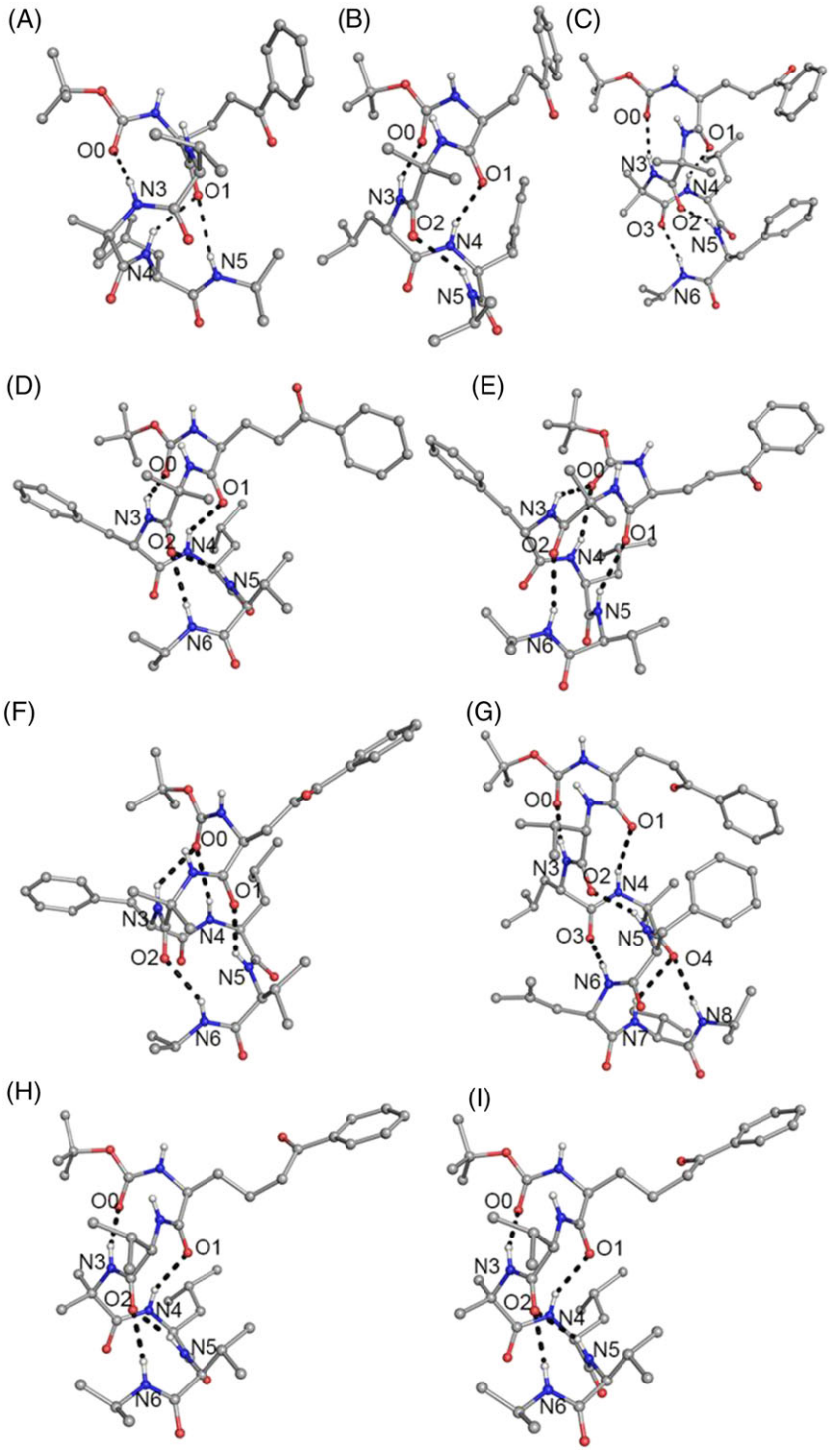

FIGURE 2 Molecular conformations of peptides **1** to **6** in crystals. A, Peptide **1**; B, peptide **2**; C, peptide **3**; D, peptide **4a** (MOL-1); E, peptide **4a** (MOL-2); F, peptide **4b**; G, peptide **5**; H, peptide **6** (MOL-1); and I, peptide **6** (MOL-2)

TABLE 1 Backbone dihedral angles of peptides **1-6**

Residues	ϕ	ψ	ω
Peptide **1**			
δOPhe	−55.9 (5)	−30.4 (6)	−179.3 (4)
Val	−56.8 (5)	−34.8 (5)	−178.3 (4)
Aib	−62.4 (5)	−27.1 (5)	−174.3 (4)
Leu	−94.0 (5)	−31.8 (5)	−171.5 (4)
Peptide **2**			
δOPhe	−56.8 (4)	−34.4 (4)	−177.8 (3)
Aib	−54.0 (4)	−34.5 (4)	−175.1 (3)
Leu	−65.8 (4)	−25.3 (4)	175.1 (3)
Phe	−63.5 (4)	−24.4 (4)	179.6 (3)
Peptide **3**			
δOPhe	−56.0 (6)	−32.5 (5)	−179.8 (4)
Aib	−48.1 (6)	−39.3 (6)	−173.7 (4)
Aib	−54.8 (5)	−32.9 (5)	−176.0 (4)
Leu	−64.3 (5)	−17.7 (6)	177.0 (4)
Phe	−93.8 (5)	−2.5 (6)	−176.1 (4)
Peptide **4a** (MOL-1)			
δOPhe	−60.0 (8)	−46.4 (8)	−176.4 (5)
Aib	−52.7 (8)	−39.3 (7)	−173.3 (5)
Phe	−73.0 (7)	−25.3 (8)	174.1 (5)
Leu	−74.0 (7)	−19.3 (8)	178.2 (6)
Val	−93.6 (7)	−43.9 (8)	171.7 (6)
Peptide **4a** (MOL-2)			
δOPhe	−60.5(7)	−36.4 (7)	179.4 (5)
Aib	−51.6 (7)	−45.1 (7)	−176.0 (5)
Phe	−77.3 (7)	−32.6 (8)	177.4 (5)
Leu	−60.0 (7)	−37.9 (7)	−177.4 (5)
Val	−86.3 (7)	−42.6 (7)	175.6 (6)
Peptide **4b**			
δOPhe	−55.9 (6)	−43.7 (6)	−177.1 (4)
Aib	−52.0 (6)	−42.4 (6)	−177.6 (4)
Phe	−78.5 (5)	−31.5 (6)	177.2 (4)
Leu	−69.6 (6)	−25.4 (6)	179.6 (4)
Val	−95.8 (5)	−59.2 (6)	178.1 (5)
Peptide **5**			
δOPhe	−65.4 (7)	−23.2 (7)	173.9 (5)
Val	−53.5 (7)	−32.2 (7)	−176.1 (5)
Leu	−55.2 (7)	−34.7 (7)	−178.1 (5)
Aib	−56.7 (6)	−29.1 (6)	−174.4 (4)
Phe	−85.1 (6)	−1.1 (7)	163.3 (5)
Leu	−78.1 (7)	−19.3 (7)	173.3 (5)
Val	−91.5 (6)	−51.8 (7)	178.4 (5)
Peptide **6** (MOL-1)			
εOPhe	−48.3 (9)	−43.7 (8)	−176.1 (5)
Val	−59.3 (8)	−24.9 (8)	178.4 (5)
Aib	−55.6 (7)	−32.8 (7)	−176.4 (5)
Leu	−78.0 (7)	−12.3 (8)	−173.2 (6)
Val	−109.4 (7)	−59.2 (7)	−179.0 (6)
Peptide **6** (MOL-2)			
εOPhe	−51.8 (8)	−42.4 (8)	−175.4 (6)
Val	−58.8 (8)	−27.4 (9)	177.9 (6)
Aib	−52.0 (8)	−37.0 (7)	−174.8 (5)
Leu	−70.3 (7)	−24.0 (8)	−172.2 (6)
Val	−99.3 (8)	−54.9 (8)	−176.1 (6)

(Continues)

TABLE 2 Intramolecular and intermolecular hydrogen bond parameters in the crystal structures of peptides **1-6** (D, donor; A, acceptor)

D—H···A	H···A, Å	D···A, Å	D—H···A, deg
Peptide **1**			
N1—H1···O3[a]	2.10	2.869 (4)	148.5
N2—H2···O1W	2.12	2.960 (5)	165.8
N3—H3···O0	2.21	2.966 (5)	146.6
N4—H4···O1	2.16	2.921 (4)	147.9
N5—H5···O1	2.36	3.100 (5)	144.1
O1W—H1w···O4[b]	1.97 (6)	2.786 (5)	173 (6)
Peptide **2**			
N1—H1···O4[c]	2.08 (4)	2.856 (4)	148 (3)
N2—H2···O4[c]	2.26	3.067 (4)	155.9
N3—H3···O0	2.33	3.103 (4)	149.6
N4—H4···O1	2.24	2.994 (4)	146.0
N5—H5···O2	2.32	3.073 (4)	146.8
Peptide **3**			
N2—H2···O4[d]	2.10	2.895 (5)	153.8
N3—H3···O0	2.20	2.999 (5)	153.5
N4—H4···O1	2.13	2.924 (5)	152.5
N5—H5···O2	2.16	2.980 (5)	160.6
N6—H6···O3	2.20	3.041 (5)	165.1
Peptide **4a** (MOL-1)			
N1—H1···O4[a]	2.08	2.865 (7)	152.4
N2—H2···O5[a]	2.07	2.848 (6)	150.0
N3—H3···O0	2.25	2.927 (7)	135.3
N4—H4···O1	2.32	2.954 (7)	130.6
N5—H5···O2	2.47	3.200 (7)	143.1
N6—H6···O2	2.11	2.969 (7)	176.7
Peptide **4a** (MOL-2)			
N1—H1···O4[e]	2.15	2.960 (6)	156.8
N2—H2···O5[e]	2.19	2.902 (6)	139.8
N3—H3···O0	2.31	2.940 (6)	130.2
N4—H4···O0	2.32	3.129 (6)	157.8
N5—H5···O1	2.30	3.099 (6)	155.5
N6—H6···O2	2.20	3.021 (6)	159.7
C1S—H1···O1D[f]	2.28	3.25 (1)	175.4
C1S—H2···O4[e]	2.34	3.227 (9)	151.2
Peptide **4b**			
N1—H1···O4[f]	2.08	2.919 (5)	166.8
N2—H2···O5[f]	2.20	2.904 (5)	139.2
N3—H3···O0	2.35	2.972 (5)	129.2
N4—H4···O0	2.27	3.082 (5)	157.1
N5—H5···O1	2.24	2.984 (5)	144.9

(Continues)

TABLE 2 (Continued)

D—H···A	H···A, Å	D···A, Å	D—H···A, deg
N6—H6···O2	2.14	2.890 (5)	145.3
O1w···O4[a]		2.830	
Peptide **5**			
N1—H1···O7[f]	2.23	3.043 (6)	158.7
N2—H2···O1S	2.02	2.870 (6)	167.8
N3—H3···O0	2.21	3.017 (6)	156.4
N4—H4···O1	2.29	3.050 (5)	147.5
N5—H5···O2	2.11	2.888 (6)	150.9
N6—H6···O3	2.14	2.953 (6)	156.9
N7—H7···O4	2.41	3.144 (6)	143.3
N8—H8···O4	2.12	2.975 (6)	173.6
O1S—H···O7[f]	1.97	2.781 (6)	169.8
Peptide **6** (MOL-1)			
N1—H1···O5[g]	2.04	2.879 (7)	164.4
N2—H2···O4[g]	2.04	2.870 (7)	162.0
N3—H3···O0	2.12	2.913 (7)	152.5
N4—H4···O1	2.14	2.929 (7)	152.6
N5—H5···O2	2.09	2.900 (7)	157.8
N6—H6···O2	2.10	2.920 (7)	158.5
Peptide **6** (MOL-2)			
N1—H1···O5[h]	2.02	2.857 (7)	165.9
N2—H2···O4[h]	2.15	2.962 (7)	158.2
N3—H3···O0	2.18	2.936 (7)	147.4
N4—H4···O1	2.18	2.955 (7)	150.4
N5—H5···O2	2.19	2.969 (7)	149.9
N6—H6···O2	2.12	2.966 (7)	168.4

[a]Symmetry code: (x, y − 1, z).
[b]Symmetry code: (x + 1, y − 1, z).
[c]Symmetry code: (x − 1, y, z).
[d]Symmetry code: (x + 1/2, y − 1/2, z).
[e]Symmetry code: (x, y + 1, z).
[f]Symmetry code: (x + 1, y, z).
[g]Symmetry code: (−x, y + 1/2, −z + 1).
[h]Symmetry code: (−x + 1, y − 1/2, −z).

while the other molecule (MOL-1) is a 3_{10}-helix with three consecutive 4 → 1 hydrogen bonds and an additional 5 → 1 hydrogen bond (N6···O2) at the C-terminus, thus providing a snapshot of the conformational transitions of the peptide in solution. The peptide conformation in polymorph **4b** is similar to that of MOL-2 in polymorph **4a**. It is evident from Tables 1 and 2 that the modified amino acid residue at the N-terminus has little effect on the secondary structure adopted by peptides **1** to **6**.

The crystal structures of peptides **1** to **6** offer seven individual conformers for the δ-oxo amino acid residue and two conformers for the ε-oxo amino acid residue. The average ϕ and ψ values observed for the δ-oxo amino acid residue are ϕ = −58.6° (±2.8°) and ψ = −35.3° (±5.9°), and those for the ε-oxo amino acid residue are ϕ = −50.1° (±1.8°) and ψ = −43.1° (±0.7°). The values of ϕ and ψ clearly indicate that the oxo amino acid residues fall well within the helical region of the Ramachandran map. An analysis of side chain conformations (Table S1) of the δ-oxo amino acid residues shows that *gauche* and *trans* conformations are equally preferred for χ^1 and χ^2, while there is a strong preference for *trans* conformation for the dihedral angle, χ^3. The preference for *trans* conformation for χ^3 is not surprising because of the presence of a bulky phenyl ring. The corresponding side chain dihedral angle (χ^4) for the ε-amino acid residue also adopts *trans* conformation. The side chain dihedral angles χ^1, χ^2, and χ^3 for the ε-amino acid residue lead to (t, t, g) conformation.

2.2.2 | Molecular packing

The molecular packing in the six peptide crystals follow the typical peptide helix packing pattern.[22,23] Helical peptides pack as columns stabilized by intermolecular head-to-tail N—H···O hydrogen bonds, which further assemble laterally through van der Waals interactions and aromatic interactions. Stereo diagrams of the overall molecular packing in the crystals of peptides **1** to **6** are provided as supporting information (Figures S1-S7).

N—H···O hydrogen-bonded head-to-tail assembly

Figure 3 summarizes the head-to-tail hydrogen-bonded motifs observed in crystals of peptides **1** to **6**. There are two intermolecular hydrogen bonds that facilitate the molecular assembly in peptide **1**: a direct N1—H···O3 (x, y − 1, z) and a water-mediated N2—H···O1W···O4 (x + 1, y − 1, z) hydrogen bonds, connecting the molecules along the crystallographic *b*- and *c*-axes, respectively (Figure 3A). Two intermolecular head-to-tail hydrogen bonds between translated molecules (N1—H···O4 [x − 1, y, z] and N2—H···O4 [x − 1, y, z]) stabilize the peptide assembly along the crystallographic *a*-axis in peptide **2** (Figure 3B). A sole intermolecular N—H···O hydrogen bond (N2—H···O4 [x + 1/2, y − 1/2, z]) stabilizes the head-to-tail assembly in the crystals of pentapeptide **3** (Figure 3C). In the polymorphs **4a** and **4b**, two sets of head-to-tail hydrogen bonds of the type N1—H···O4 and N2—H···O5 stabilize the packing of helices into columns (Figure 3D,E). The polymorph **4a**, which has a co-crystallized dichloromethane molecule in the asymmetric unit, possesses two C—H···O hydrogen bonds originating from the solvent molecule (C—H···O4 and C—H···O1D). A direct N1—H···O7 (x + 1, y, z) hydrogen bond and a solvent-mediated N2—H···O1S···O7 (x + 1, y, z) hydrogen bond are observed in the head-to-tail assembly of heptapeptide **5** in crystals (Figure 3F). In peptide **6**, molecules related by the 2_1-screw symmetry along the crystallographic *b*-axis are connected through N1—H···O5 and N2—H···O4 intermolecular hydrogen bonds (Figure 3G).

Aromatic interactions

The availability of aromatic rings on the side chains of the oxo amino acid and the Phe residues enables the stabilization of molecular conformations and packing by aromatic interactions. A summary of the aromatic interactions observed in the peptide crystals is provided in Figure 4. Relevant parameters for defining the aromatic interactions, namely, the centroid···centroid distance (R_{cent}), shortest (phenyl) C···C(phenyl) distance (R_{clo}), and the interplanar angle (γ) of the interacting aromatic rings are summarized in Table S3. Intermolecular aromatic interactions between hydrogen-bonded molecules along the crystallographic *a*-axis (R_{cent} = 5.0 Å, R_{clo} = 3.4 Å, γ = 28.1°) and

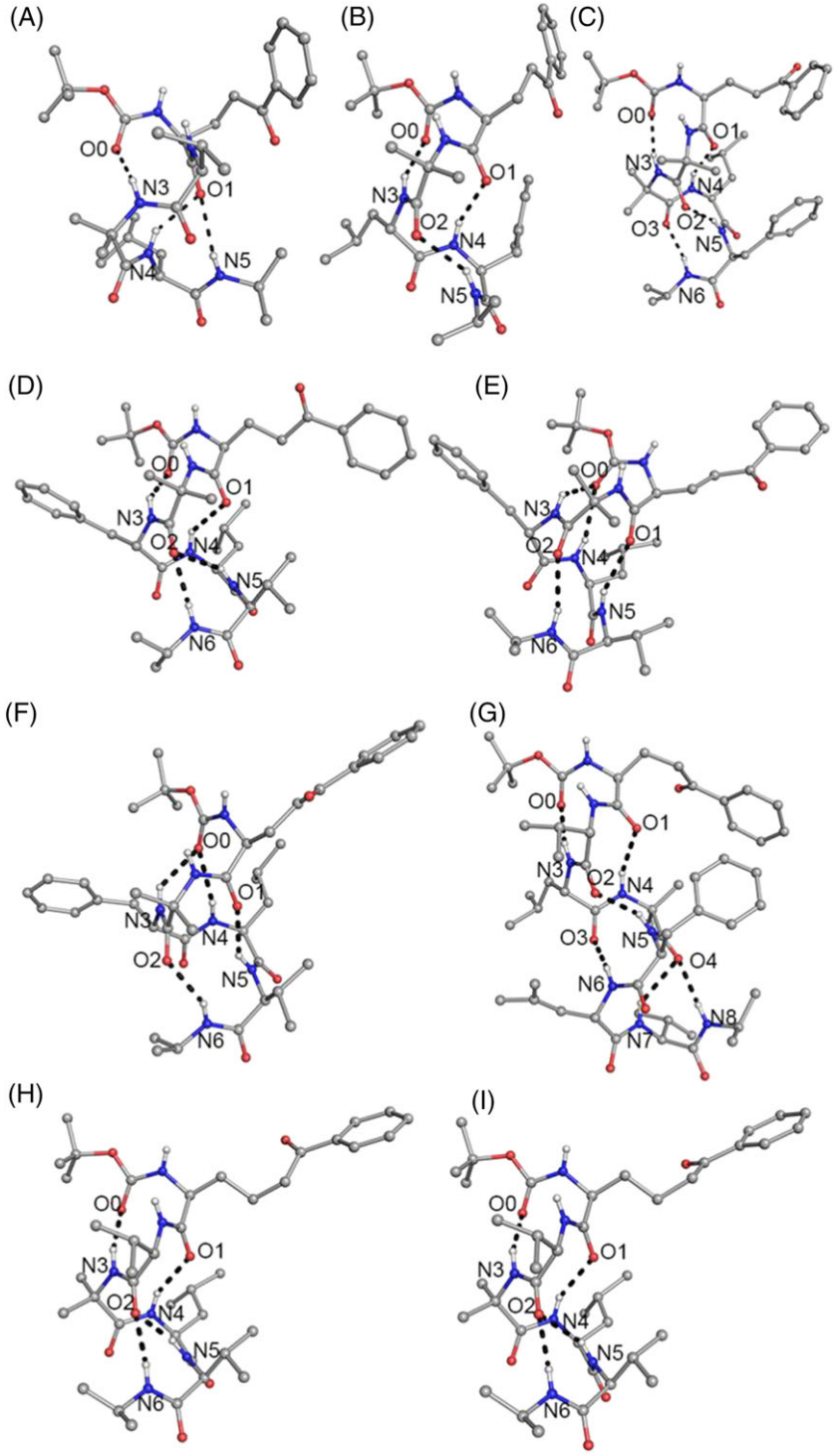

FIGURE 3 Intermolecular N—H···O interactions in the crystals of peptides **1** to **6**. A, Peptide **1**; B, peptide **2**; C, peptide **3**; D, peptide **4a** (MOL-1); E, peptide **4b**; F, peptide **5**; and G, peptide **6** (MOL-1). For peptides **4a** and **6**, which have two molecules in the asymmetric unit, one of the molecules is depicted

between the 2_1-screw related molecules along the crystallographic *c*-axis (R_{cent} = 4.1 Å, R_{clo} = 3.3 Å, γ = 21.1°) stabilize molecular packing in peptide **2** (Figure 4A). In peptide **3**, centroids of the aromatic rings of residue 1 and residue 5 are 6 Å apart (R_{clo} = 4.0 Å, γ = 57.2°), suggesting a weak intramolecular aromatic interaction. Extensive intermolecular aromatic interactions are observed in the packing of peptide **3**, as shown in Figure 4B. The strongest interaction in this case is between residue 1 side chains of molecules related by a twofold rotation (R_{cent} = 5.3 Å, R_{clo} = 3.7 Å, γ = 27.1°). In the polymorph **4a**, the centroid of the aromatic ring of the oxo residue of MOL-2 is 5.4 Å away from that of the Phe residue of MOL-1 (Figure 4C, R_{clo} = 4.1 Å, γ = 76.2°), while two sets of intermolecular aromatic interactions between residues 4 and 1 are observed in the polymorph **4b** (Figure 4D, R_{cent} = 5.1 Å, R_{clo} = 4.4 Å, γ = 83.3° and R_{cent} = 5.4 Å, R_{clo} = 3.8 Å, γ = 50.2°). In peptide **5**, the *gauche* conformation adopted by χ^2 of the δ-oxo amino acid residue facilitates a strong intramolecular π-π interaction with a centroid···centroid distance of 4.9 Å (R_{clo} = 3.7 Å, γ = 73.4°). Adjacent helices related by the symmetry (*x*, *y* + 1, *z*) are connected through an intermolecular π-π interaction between residues 1 and 4 with a centroid···centroid distance of

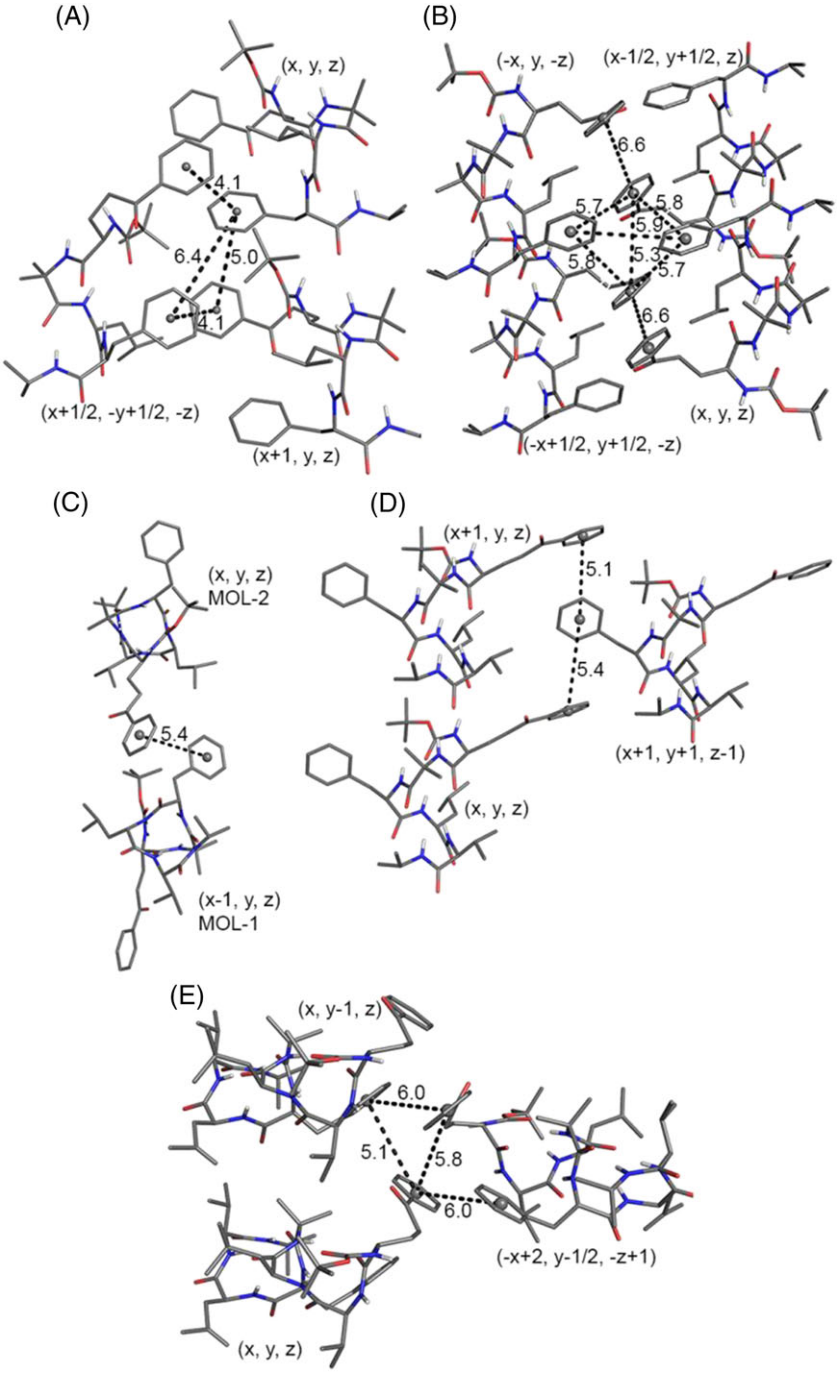

FIGURE 4 Intermolecular aromatic interactions in peptides **2** to **5**. A, Peptide **2**; B, peptide **3**; C, peptide **4a**; D, peptide **4b**; E, peptide **5**. Centroid···centroid distance (Å) between the interacting rings and the symmetry relation between the interacting molecules are marked

5.1 Å (R_{clo} = 3.9 Å, γ = 73.2°). Longer interaction distances (5.8 and 6.0 Å) between molecules related by 2_1-screw symmetry are also observed in the molecular packing of peptide **5** (Figure 4E). No aromatic interactions are observed in peptides **1** and **6**. Depending on the interplanar angle of interacting aromatic rings, the interactions can be classified into π···π stacking (γ ~ 0°), edge-to-face (γ ~ 90°), and inclined (0 < γ < 90°). In the present study, an edge-to-face geometry is observed in peptide **4b** (γ = 83.3°, R_{cent} = 5.1 Å). The values of γ between 70° and 80°, observed in peptides **3** (R_{cent} = 5.9 Å), **4a**, and **5** (R_{cent} = 5.1 and 5.8 Å), also indicate an approximately edge-to-face aromatic pair. Only one example of a parallel displaced (π···π stacking) arrangement is observed (peptide **5**, R_{cent} = 6.0 Å, γ = 2.1°). The remaining interactions can be classified as inclined, with values of γ between 20° and 60°.

C—H···O interactions of oxo amino acid side chains

Table 3 and Figure 5 summarize the short intermolecular C···O contacts originating from the side chain atoms of δ- and ε-oxo amino acid residues. Although most of the H···O distances are at the borderline to be considered as C—H···O hydrogen bonds, an analysis of the interactions could be useful in determining the possible modes of molecular aggregation through these modified side chains. Interestingly, all the interactions observed are intermolecular, suggesting that these residues are not altering the secondary structures of the peptides. A

TABLE 3 Intermolecular C—H···O contacts of side chains of the oxo amino acid residues

	D—H···A	H···A, Å	D···A, Å	D—H···A, deg
Peptide **1**	C1F—H···O2[a]	2.54	3.411 (6)	155.7
Peptide **2**	C1I—H···O0[b]	2.63	3.506 (5)	156.3
Peptide **3**	C1B—H···O1D[c]	2.52	3.403 (6)	151.0
Peptide **4a**	C11B—H···O51[a] C12G—H···O42[d] C12B—H···O52[d]	2.62 2.56 2.58	3.469 (8) 3.395 (8) 3.517 (8)	146.1 145.4 162.7
Peptide **4b**	C1B—H···O5[e]	2.51	3.403 (6)	152.9
Peptide **6**	C11D—H···O13[f] C11L—H···O23[g] C21D—H···O23[h] C21L—H···O13[i]	2.36 2.59 2.43 2.65	3.313 (8) 3.328 (9) 3.265 (8) 3.413 (8)	166.9 136.9 144.1 139.5

[a]Symmetry code: (*x*, *y* − 1, *z*).

[b]Symmetry code: (*x* − 1/2, −*y* + 3/2, −*z*).

[c]Symmetry code: (−*x* + 1, *y*, −*z*).

[d]Symmetry code: (*x*, *y* + 1, *z*).

[e]Symmetry code: (*x* + 1, *y*, *z*).

[f]Symmetry code: (−*x*, *y* + 1/2, −*z* + 1).

[g]Symmetry code: (*x*, *y*, *z* + 1).

[h]Symmetry code: (−*x* + 1, *y* − 1/2, −*z*).

[i]Symmetry code: (*x*, *y*, *z*).

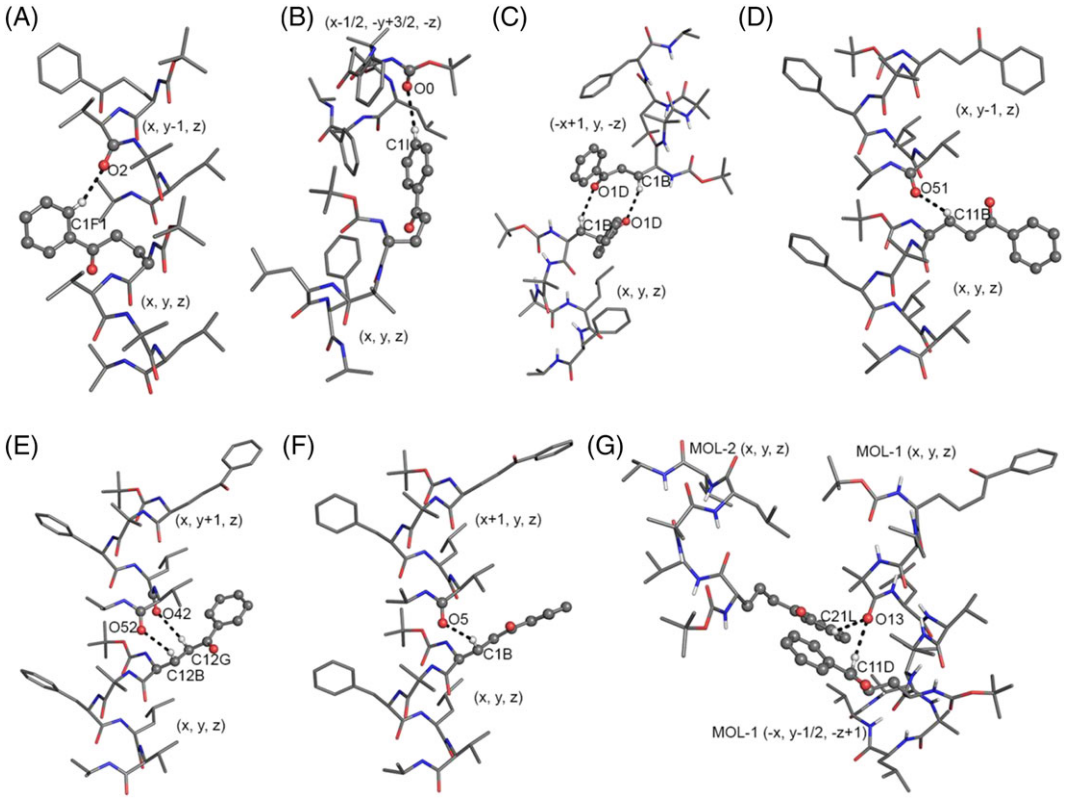

FIGURE 5 Intermolecular C—H···O contacts observed in the crystals of peptides **1** to **6**. A, Peptide **1**; B, peptide **2**; C, peptide **3**; D, peptide **4a** (MOL-1); E, peptide **4a** (MOL-2); F, peptide **4b**; and G, peptide **6**. As similar types of interactions are observed for MOL-1 and MOL-2 in **6**, only a representative set of interactions are shown

close inspection of Table 3 and Figure 5 leads to the following observations:

1. The C—H···O contacts are present both in the columnar assembly and in the lateral assembly of helices.
2. The C—H···O interactions observed in peptides **1** to **6** could be of two types: (a) interactions between side chain C—H groups of the oxo amino acid residue and the backbone carbonyl oxygen atoms and (b) interactions between side chain C—H groups and carbonyl oxygen atoms of the oxo side chain.

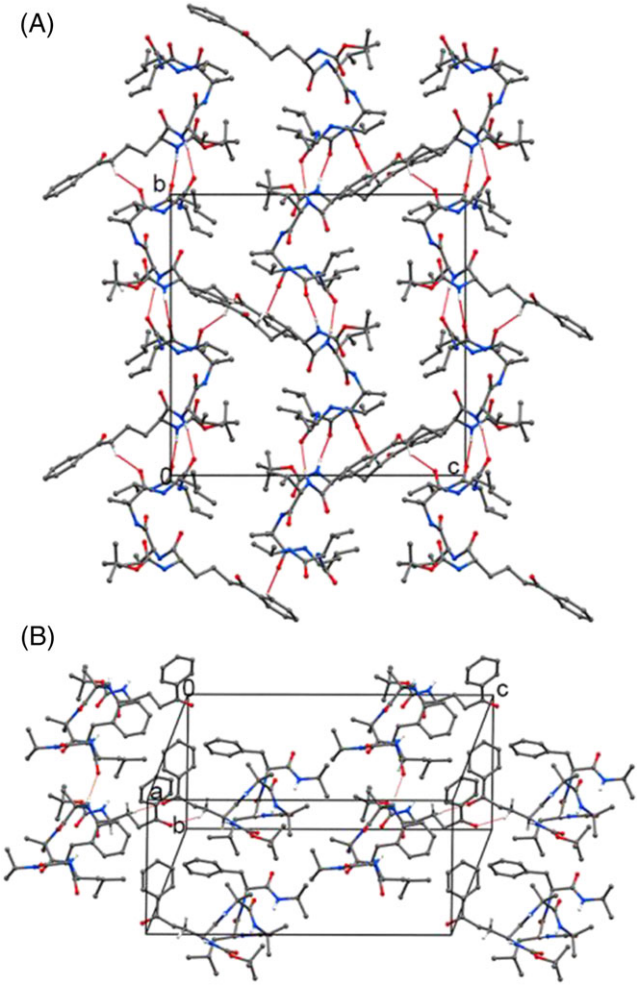

FIGURE 6 A, Molecular packing of peptide **6**, viewed down the crystallographic *a*-axis, showing the side chain–backbone C—H···O interaction in the head-to-tail assembly of helices. Molecules related by the 2_1-screw symmetry are connected through two N—H···O hydrogen bonds and a C—H···O interaction. B, Molecular packing of peptide **3**, showing side chain–side chain C—H···O interaction in the lateral association of helices. Intermolecular hydrogen bonds are denoted by dotted lines in red color

3. In category b, two modes of side chain–backbone associations are observed: one in which the C—H···O interactions are between molecules that are already connected through head-to-tail N—H···O hydrogen bonds and another in which the C—H···O interactions are between helices that are connected laterally through aromatic π···π interactions. In the former case, the side chain–backbone C—H···O interactions offer additional stabilization to the head-to-tail hydrogen-bonded columns of helices. A representative packing diagram (of peptide **6**) is provided in Figure 6A. In peptides **1** and **6**, the backbone carbonyl oxygen atom (O2 in **1**, O3 in **6**), which is rendered free for hydrogen bonding by the formation of a 5 → 1 hydrogen bond at the C-terminus of the peptide (Figure 5A,F; Table 2), is the acceptor of C—H···O hydrogen bond interactions. Peptides **4** and **5** show C—H···O contacts to the backbone carbonyl oxygen atoms already involved in head-to-tail N—H···O hydrogen bonds (Figure 5D,E). C—H···O contacts belonging to the latter type are observed in peptides **2** (C1I···O0) and **6** (C11L···O23), facilitating the lateral association of helices (Figure 5B,G).
4. C—H···O interactions belonging to category b are observed in the crystals of peptide **3**, which provides a unique example of side chain–side chain C—H···O contact. In peptide **3**, intermolecular C—H···O interactions are observed between the side chain δ-carbonyl group and the C^{β}-hydrogen atom of molecules related by the twofold rotation (−*x* + 1, *y*, −*z*) as depicted in Figure 5C. A packing diagram of peptide **3** shown in Figure 6B illustrates this interaction in the lateral association of helices.

A comparison of the side chain torsion angle C(ortho)—C(ipso)—C=O of the oxo amino acid residues (Table S4) shows that the value of this torsion angle is slightly larger in peptides **3** (21.8°) and **5** (−23°). This could make the keto carbonyl group sterically less hindered by the vicinal phenyl ring and facilitate intermolecular hydrogen bonding through the carbonyl oxygen atom. However, the absence of interactions originating from the keto group in peptide **5** indicates that the steric factor alone is not the determinant of the unique hydrogen bond observed in peptide **3**. Notably, an aromatic interaction with an interaction distance of 5.3 Å exists between the oxo amino acid side chains in this case.

5. Peptide **5** does not show any C—H···O interactions involving the oxo amino acid residue.

3 | CONCLUSIONS

We have introduced an isolated carbonyl functionality in the side chain at the N-terminus of oligopeptides to examine the possibilities of increasing the intermolecular contacts for self-assembly of these peptides. Crystal structure analysis of the six peptides shows that these peptides adopted helical structures in crystals. Incorporating an oxo amino acid residue at the N-terminus favors interactions between side chain C—H and backbone carbonyl groups in a head-to-tail assembly of helices. The tendency of the side chain C—H of oxo residues to act as an H-bond donor is due to the presence of the adjacent carbonyl group, which makes the C—H more acidic. In the present study, intermolecular interactions originating from the oxo amino acid side chains appear to be present only in combination with additional directional interactions such as aromatic interactions and N—H···O hydrogen bonds. The side chain–side chain interaction observed between the laterally positioned helices of peptide **3** is suggestive of its possible utilization in directing lateral self-assembly of peptide helices through side chain association. We believe that further studies using these unusual amino acids can establish them as tools for introducing additional intermolecular interactions in synthetic peptides.

4 | EXPERIMENTAL SECTION

4.1 | Chemicals and equipment

All the chemicals were purchased from commercial sources and were used without further purification. Anhydrous THF or anhydrous

dichloromethane (DCM) were used as solvents for the reactions under nitrogen atmosphere. Thin-layer chromatography (TLC) was performed on precoated aluminum sheets (TLC silica gel 60 F254). The spots were visualized under ultraviolet (UV) light or through iodine or ninhydrin staining. Column chromatography was performed using 100- to 200-mesh silica gel and using mixtures of petroleum ether and ethyl acetate as eluent. ^{1}H nuclear magnetic resonance (NMR) and ^{13}C NMR spectra in $CDCl_3$ were recorded on a JEOL-ECX 500 FT NMR machine at 500 and 125 MHz, respectively, or on a JEOL-ECX 400 FT NMR machine at 400 and 100 MHz, respectively. The ^{1}H NMR signals are referenced to tetramethylsilane (δ = 0.00 ppm), and the ^{13}C NMR peaks are referenced to residual $CHCl_3$ signal (δ = 77.0 ppm). Chemical shifts are quoted in parts per million (ppm), and coupling constants (J) are quoted in hertz, and the observed signal multiplicities are reported as s = singlet, d = doublet, t = triplet, q = quartet, and m = multiplet and as dd = doublet of a doublet, ddd = doublet of a doublet of a doublet, dt = doublet of a triplet, and dq = doublet of a quartet. High-resolution electrospray ionization (ESI) mass spectra were recorded on a WATERS Q-TOF premier mass spectrometer (Milford, Massachusetts). Infrared spectra (FT-IR) were recorded on a Perkin-Elmer model 1320 spectrometer (Waltham, Massachusetts) including a diamond universal ATR sampling technique (attenuated total reflectance) from 4000 to 400 cm^{-1}. The absorption bands are reported in wave numbers (cm^{-1}).

4.2 | Synthesis of the oxo amino acid derivatives 11a and 11b

The two unnatural amino acid derivatives **11a** (δ-oxo δ-phenyl α-amino acid derivative) and **11b** (ε-oxo ε-phenyl α-amino acid derivative) were synthesized from the iodide derivatives **7a** and **7b**, respectively, by the extension of a procedure that we had developed (Scheme 1).

4.2.1 | Synthesis of compounds 8a and 8b from 7a and 7b

The dithiane derivative of benzaldehyde (0.98 g, 5 mmol) was dissolved in anhydrous THF (10 mL), and the solution was cooled to −50 °C. *n*-BuLi (3.4 mL, 5.5 mmol, 1.6M in hexane) was added dropwise to this solution. When the reaction mixture turned orange in color (indicating the formation of the anion), the iodide **7a** or **7b** (3.5 mmol) in THF (5 mL) was added over a period of 15 minutes, and the stirring was continued. The reaction was monitored by TLC until the complete disappearance of **7**. The reaction was quenched with a saturated solution of NH_4Cl and extracted with Et_2O (2 × 30 mL). The organic layer was over anhydrous Na_2SO_4, and the solvent was removed under vacuum. The crude product **8** was purified by column chromatography.

Compound 8a

Column chromatography (petroleum ether/EtOAc, 96:4); white solid (1.8 g, 85%); mp 105 °C; infrared (IR) (KBr) $\overline{\nu}_{max}$ (cm^{-1}): 2932, 1696, 1386, 1256; ^{1}H NMR (500 MHz, $CDCl_3$): δ 7.88 (s, 2H), 7.38 to 7.23 (m, 3H), 3.83 (s, 1H), 3.62 to 3.59 (m, 2H), 3.28 to 3.17 (m, 1H), 2.56 (m, 4H), 2.08 to 1.82 (m, 4H), 1.71 (s, 1H), 1.59 to 1.10 (m, 16H), 0.86 (s, 1H); ^{13}C NMR (125 MHz, $CDCl_3$): δ 151.8, 141.6, 131.5, 128.7, 127.0, 93.7, 79.6, 67.3, 58.7, 57.1, 42.0, 28.6, 28.3, 27.7, 26.7, 25.1, 23.2; (HRMS) (ESI): *m/z* calcd for $C_{22}H_{34}NO_3S_2$ $[M + H]^+$: 424.1980, found: 424.1985.

Compound 8b

Column chromatography (petroleum ether/EtOAc, 96:4); white solid (1.8 g, 84%); mp 110 °C; IR (KBr) $\overline{\nu}_{max}$ (cm^{-1}): 2980, 1690, 1386, 1256; ^{1}H NMR (500 MHz, $CDCl_3$): δ 7.90 (s, 2H), 7.38 (s, 2H), 7.26 (s, 1H), 3.81 (s, 1H), 3.61 (m, 2H), 2.69 (s, 4H), 2.00 (m, 2H), 1.95 (s, 2H), 1.66 (s, 2H), 1.53 to 1.42 (m, 15H), 1.25 (m, 2H); ^{13}C NMR (125 MHz, $CDCl_3$): δ (mixture of rotamers) 151.9, 141.4, 129.0, 129.0, 93.6, 93.1, 80.0, 79.5, 67.1, 66.3, 61.3, 59.0, 57.6, 57.0, 45.2, 44.9, 33.9, 32.4, 28.5, 27.7, 26.8, 25.3, 24.6, 23.2, 20.8; HRMS (ESI): *m/z* calcd for $C_{23}H_{36}NO_3S_2$ $[M + H]^+$: 438.2137, found: 438.2140.

4.2.2 | Acidolysis of the oxazolidine ring in 8a and 8b to get 9a and 9b

The oxazolidine **8a** or **8b** (4.2 mmol) was cooled to 0 °C, and a solution of TFA (7%) in methanol (5 mL) was added drop wise. The reaction was monitored by TLC, and on complete disappearance of **8**, the reaction was quenched with $NaHCO_3$ (1 g). The solution was filtered, and the filtrate was concentrated under vacuum. The crude amino alcohol derivative **9** was purified by column chromatography.

Compound 9a

Column chromatography (petroleum ether/EtOAc, 75:25); colorless oil (1.38 g, 88%); IR (thin film) $\overline{\nu}_{max}$ (cm^{-1}): 3375, 2975, 1694, 1386, 1256; ^{1}H NMR (500 MHz, $CDCl_3$): δ 7.85 (d, J = 7.5 Hz, 2H), 7.35 (t, J = 7.7 Hz, 2H), 7.23 (t, J = 7.3 Hz, 1H), 4.61 (s, 1H), 3.48 (d, J = 10.1 Hz, 1H), 3.37 (d, J = 10.6 Hz, 1H), 2.82 (s, 1H), 2.66 (s, 4H), 2.10 to 2.01 (m, 2H), 1.90 (s, 2H), 1.38 (s, 11H); ^{13}C NMR (125 MHz, $CDCl_3$): δ 156.5, 141.6, 128.7, 127.1, 79.7, 65.7, 58.6, 52.6, 41.4, 28.4, 27.6, 26.0, 25.2; HRMS (ESI): *m/z* calcd for $C_{19}H_{30}NO_3S_2$ $[M + H]^+$: 384.1667, found: 384.1670.

Compound 9b

Column chromatography (petroleum ether/EtOAc, 75:25); colorless oil (1.39 g, 85%); IR (thin film) $\overline{\nu}_{max}$ (cm^{-1}): 3370, 2978, 1690, 1386, 1256; ^{1}H NMR (500 MHz, $CDCl_3$): δ 7.88 (d, J = 8.0 Hz, 2H), 7.35 (d, J = 7.3 Hz, 2H), 7.23 (d, J = 7.3 Hz, 1H), 4.52 (s, 1H), 3.55 (s, 1H), 3.48 (s, 1H), 3.42 (s, 1H), 2.66 (s, 4H), 2.04 to 1.90 (m, 4H), 1.74 (s, 2H), 1.40 (s, 9H), 1.32 (m, 2H); ^{13}C NMR (125 MHz, $CDCl_3$): δ 156.5, 141.7, 128.8, 128.6, 127.0, 79.7, 65.8, 59.0, 52.5, 44.9, 31.4, 28.4, 27.7, 25.3, 20.6; HRMS (ESI): *m/z* calcd for $C_{20}H_{32}NO_3S_2$ $[M + H]^+$: 398.1824, found: 398.1818.

4.2.3 | Hydrolysis of the dithiane groups in 9a and 9b to get 10a and 10b

To a solution of the dithiane derivative **9a** or **9b** (3.6 mmol) in acetonitrile (5 mL), saturated $NaHCO_3$ solution (5 mL) was added, the mixture was cooled to 0 °C, and iodine (3.65 g, 14.34 mmol) was added

in small portions. The reaction mixture was stirred vigorously and allowed to attain room temperature. After 1 hour, reaction was quenched by adding a saturated solution of $Na_2S_2O_3$ (5 mL), and the product was extracted with diethyl ether (3 × 20 mL). The crude solution was washed with brine, dried with anhydrous Na_2SO_4, concentrated under vacuum, and purified by column chromatography.

Compound 10a

Column chromatography (petroleum ether/EtOAc, 70:30); white solid (0.949 g, 90%); mp 80 °C; IR (thin film) $\overline{\nu}_{max}$ (cm^{-1}): 3360, 1680, 1586, 1256; ^1H NMR (500 MHz, $CDCl_3$): δ 7.93 (d, *J* = 8.5 Hz, 2H), 7.53 (t, *J* = 7.4 Hz, 1H), 7.43 to 7.40 (m, 2H), 5.02 (d, *J* = 8.6 Hz, 1H), 3.67 to 3.63 (m, 2H), 3.58 to 3.55 (m, 1H), 3.08 (s, 2H), 2.03 to 1.95 (m, 1H), 1.90 (s, 1H), 1.37 (s, 9H); ^{13}C NMR (125 MHz, $CDCl_3$): δ 200.4, 156.4, 136.7, 133.3, 128.7, 128.2, 79.6, 65.2, 52.5, 35.3, 28.4, 25.5; HRMS (ESI): *m/z* calcd for $C_{16}H_{23}NNaO_4$ $[M + Na]^+$: 316.1525, found: 316.1519.

Compound 10b

Column chromatography (petroleum ether/EtOAc, 70:30); white solid; mp 78 °C; (0.969 g, 90%); IR (thin film) $\overline{\nu}_{max}$ (cm^{-1}): 3365, 1680, 1586, 1256; ^1H NMR (500 MHz, $CDCl_3$): δ 7.94 (d, *J* = 8.5 Hz, 2H), 7.55 (t, *J* = 7.4 Hz, 1H), 7.45 (t, *J* = 7.7 Hz, 2H), 4.83 (s, 1H), 3.68 to 3.62 (d, 3H), 3.08 to 2.95 (m, 2H), 1.86 to 1.75 (m, 2H), 1.62 to 1.59 (m, 1H), 1.53 (s, 1H), 1.43 (s, 9H); ^{13}C NMR (125 MHz, $CDCl_3$): δ 200.3, 156.6, 136.9, 133.2, 128.7, 128.1, 79.7, 65.8, 52.6, 38.0, 30.9, 28.5, 20.4; HRMS (ESI): *m/z* calcd for $C_{17}H_{25}NNaO_4$ $[M + Na]^+$: 330.1681, found: 330.1678.

4.2.4 | Oxidation of 10a and 10b to 11a and 11b

The *N*-Boc amino alcohol derivative **10a** or **10b** (3 mmol) was dissolved in anhydrous DMF (15 mL), and pyridinium dichromate (11.28 g, 30 mmol) was added at room temperature. The reaction mixture was stirred for 12 hours, and then water (10 mL) was added to quench the reaction. The amino acid derivative was extracted from the crude solution with diethyl ether (3 × 25 mL); the ether solutions were pooled together, washed with brine (3 × 25 mL), dried over anhydrous Na_2SO_4, and concentrated under reduced pressure. The crude product was purified by column chromatography.

Compound 11a

Column chromatography (petroleum ether/EtOAc, 50:50); white solid (0.649 g, 70%); mp 84 °C; IR (thin film) $\overline{\nu}_{max}$ (cm^{-1}): 3350 (br), 1720, 1576, 1156; ^1H NMR (500 MHz, $CDCl_3$): δ 7.96 (s, 2H), 7.55 (s, 1H), 7.44 (s, 2H), 5.30 (s, 1H), 4.39 (s, 1H), 3.18 (s, 1H), 3.12 (s, 1H), 2.35 (s, 1H), 2.14 (s, 1H), 1.41 (s, 9H); ^{13}C NMR (125 MHz, $CDCl_3$): δ 199.8, 175.8, 163.3, 136.6, 133.4, 128.7, 128.2, 80.4, 53.1, 36.9, 34.8, 31.8, 28.3, 26.9; HRMS (ESI): *m/z* calcd for $C_{16}H_{21}NNaO_5$ $[M + Na]^+$: 330.1317, found: 330.1310.

Compound 11b

Column chromatography (petroleum ether/EtOAc, 50:50); white solid (0.649 g, 70%); mp 82 °C; IR (thin film) $\overline{\nu}_{max}$ (cm^{-1}): 3360 (br), 1720, 1576, 1156; ^1H NMR (500 MHz, $CDCl_3$): δ 7.94 (d, *J* = 7.6 Hz, 2H), 7.55 (t, *J* = 7.3 Hz, 1H), 7.44 (t, *J* = 7.6 Hz, 2H), 5.84 (s, 1H), 5.25 (d, *J* = 5.1 Hz, 1H), 4.36 (s, 1H), 3.04 (s, 2H), 1.95 to 1.83 (m, 4H), 1.44 (s, 9H); ^{13}C NMR (125 MHz, $CDCl_3$): δ 200.1, 176.4, 155.9, 136.8, 133.3, 128.7, 128.2, 80.3, 53.2, 37.8, 31.8, 28.4, 19.8; HRMS (ESI): *m/z* calcd for $C_{17}H_{23}NNaO_5$ $[M + Na]^+$: 344.1474, found: 344.1470.

4.3 | Peptide synthesis

Peptides **1** to **6** were synthesized by conventional solution-phase peptide synthesis of *N*-Boc residues and *C*-methyl–protected residues. Coupling of **11a** with H-Val-Aib-Leu-NH^{i}Pr, H-Aib-Leu-Phe-NH^{i}Pr, H-Aib-Aib-Leu-Phe-NH^{i}Pr, H-Aib-Phe-Leu-Val-NH^{i}Pr, and H-Val-Leu-Aib-Phe-Leu-Val-NH^{i}Pr gave peptides **1** to **5**, respectively. Peptide **6** was prepared by coupling **11b** with H-Val-Aib-Leu-Val-NH^{i}Pr.

4.3.1 | General procedure

The amino acid derivative **11a** or **11b** (0.68 mmol) was dissolved in dichloromethane (10 mL) and was cooled in an ice bath. EDC·HCl (0.20 g, 1.04 mmol) and HOBt (0.14 g, 1.02 mmol) were added to this solution. After the mixture was stirred for 10 minutes, the required *C*-protected peptide fragment (0.68 mmol) was added to this solution, which was followed with the addition of *N*,*N*-diisopropylethylamine (DIPEA) (0.22 mL, 1.25 mmol). The mixture was stirred at room temperature for 10 hours and then diluted with dichloromethane (20 mL). The resultant solution was washed with brine (2 × 20 mL), 2N HCl (2 × 20 mL) and saturated $NaHCO_3$ (2 × 20 mL) and was dried over anhydrous Na_2SO_4. The solvents were evaporated to get the desired oxo peptides, which were purified by column chromatography.

Boc-δOPhe-Val-Aib-Leu-NH^{i}Pr (1)

Column chromatography (petroleum ether/EtOAc, 40:60); white solid (0.300 g, 69%); mp 220 °C; IR (KBr) $\overline{\nu}_{max}$ (cm^{-1}): 3371, 2970, 1661 (br), 1511, 1457, 1480, 1336, 1254, 1171; ^1H NMR (500 MHz, $CDCl_3$) δ 7.95 (d, *J* = 7.4 Hz, 2H), 7.60 (t, *J* = 7.4 Hz, 1H), 7.48 (t, *J* = 7.7 Hz, 2H), 7.38 (s, 1H), 7.05 (d, *J* = 7.7 Hz, 1H), 6.90 (d, *J* = 7.9 Hz, 1H), 6.72 (d, *J* = 4.7 Hz, 1H), 6.16 (s, 1H), 4.32 to 4.27 (m, 1H), 4.03 to 3.99 (m, 1H), 3.93 to 3.89 (m, 2H), 3.34 to 3.25 (m, 1H), 3.20 to 3.14 (m, 1H), 2.29 to 2.25 (m, 1H), 2.23 to 2.19 (m, 1H), 1.87 (s, 2H), 1.64 to 1.60 (m, 2H), 1.57 (s, 3H), 1.45 (d, *J* = 13.3 Hz, 12H), 1.17 (d, *J* = 6.5 Hz, 3H), 1.13 (d, *J* = 6.5 Hz, 3H), 0.97 (dd, *J* = 13.4, 6.9 Hz, 6H), 0.90 (d, *J* = 6.4 Hz, 3H), 0.86 (d, *J* = 6.4 Hz, 3H); ^{13}C NMR (125 MHz, $CDCl_3$) δ 200.3, 174.2, 173.4, 171.8, 170.8, 156.9, 136.2, 133.9, 128.9, 128.2, 81.4, 60.8, 57.5, 57.0, 52.5, 41.3, 40.2, 35.5, 28.9, 28.3, 27.6, 25.3, 25.0, 23.7, 23.5, 22.5, 21.0, 19.3, 17.6; HRMS (ESI): *m/z* calcd for $C_{34}H_{56}N_5O_7$ $[M + H]^+$: 646.4180, found: 646.4176.

Boc-δOPhe-Aib-Leu-Phe-NH^{i}Pr (2)

Column chromatography (petroleum ether/EtOAc, 40:60); white solid (0.520 g, 85%); mp 180 °C; IR (KBr) $\overline{\nu}_{max}$ (cm^{-1}): 3311, 2978, 1671 (br), 1531, 1467, 1450, 1336, 1254, 1171; ^1H NMR (400 MHz, $CDCl_3$) δ 7.93 (d, *J* = 7.5 Hz, 2H), 7.59 (t, *J* = 7.4 Hz, 1H), 7.48 to 7.42 (m, 3H), 7.26 to 7.22 (m, 2H), 7.19 to 7.08 (m, 4H), 6.78 (s, 1H), 6.73

(d, *J* = 7.9 Hz, 1H), 6.12 (s, 1H), 4.60 (t, *J* = 10.3 Hz, 1H), 4.11 to 3.99 (m, 2H), 3.80 (t, *J* = 6.6 Hz, 1H), 3.47 (dd, *J* = 14.2, 3.3 Hz, 1H), 3.29 to 3.19 (m, 1H), 3.15 to 3.08 (m, 1H), 2.87 to 2.79 (m, 1H), 2.17 (s, 2H), 1.82 (s, 2H), 1.60 to 1.57 (m, 1H), 1.53 (s, 3H), 1.46 (s, 9H), 1.40 (s, 3H), 1.17 (d, *J* = 6.5 Hz, 3H), 1.12 (d, *J* = 6.5 Hz, 3H), 0.83 (d, *J* = 6.4 Hz, 3H), 0.77 (d, *J* = 6.5 Hz, 3H); ^{13}C NMR (125 MHz, $CDCl_3$) δ 200.0, 175.0, 172.7, 172.4, 170.6, 156.9, 138.7, 136.3, 133.8, 129.3, 128.8, 128.1, 126.1, 81.2, 57.3, 56.7, 54.6, 53.9, 41.5, 39.6, 37.0, 35.3, 28.2, 27.7, 24.9, 23.5, 23.0, 22.6, 22.4, 20.9; HRMS (ESI): *m/z* calcd for $C_{38}H_{56}N_5O_7$ $[M + H]^+$: 694.4180, found: 694.4177.

Boc-δOPhe-Aib-Aib-Leu-Phe-NH^{i}Pr (3)

Column chromatography (petroleum ether/EtOAc, 20:80); white solid (0.350 g, 70%); mp 122 °C; IR (KBr)$\overline{\nu}_{max}$ (cm^{-1}): 3341, 3293, 2925, 1686, 1695, 1660,1644, 1540, 1465, 1268; ^{1}H NMR (500 MHz, $CDCl_3$): δ 7.96 (d, *J* = 8.3 Hz, 2H), 7.61 (t, *J* = 7.3 Hz, 1H), 7.48 (dd, *J* = 15.1, 7.2 Hz, 5H), 7.27 (d, *J* = 6.8 Hz, 3H), 7.15 (t, *J* = 7.5 Hz, 2H), 7.07 (t, *J* = 7.3 Hz, 1H), 6.97 (d, *J* = 7.8 Hz, 1H), 6.85 (s, 1H), 6.17 (s, 1H), 4.72 to 4.60 (m, 1H), 4.06 to 4.03 (m, 2H), 3.83 (s, 1H), 3.55 (d, *J* = 14.5 Hz, 1H), 3.31 to 3.26 (m, 1H), 3.18 to 3.14 (m, 1H), 2.93 to 2.87 (m, 1H), 2.19 to 2.16 (m, 2H), 1.61 to 1.55 (m, 1H), 1.67 (s, 1H), 1.53 (s, 3H), 1.47 (s, 10H), 1.41 (s, 3H), 1.38 (s, 3H), 1.25 (s, 3H), 1.18 (t, *J* = 6.4 Hz, 6H), 0.87 (d, *J* = 6.4 Hz, 3H), 0.80 (d, *J* = 6.6 Hz, 3H); ^{13}C NMR (125 MHz, $CDCl_3$): δ 199.9, 176.1, 174.4, 173.1, 172.5, 170.8, 156.8, 138.9, 136.2, 133.9, 129.2, 129.0, 128.1, 126.0, 81.3, 57.3, 57.0, 56.7, 54.5, 54.2, 41.6, 39.2, 38.7, 37.1, 35.3, 29.7, 28.3, 27.6, 25.0, 23.2, 22.6, 22.3, 20.9; HRMS (ESI): *m/z* calcd for $C_{42}H_{63}N_6O_8$ $[M + H]^+$: 779.4707, found: 779.4698.

Boc-δOPhe-Aib-Phe-Leu-Val-NH^{i}Pr (4)

Column chromatography (petroleum ether/EtOAc, 20:80); white solid (0.320 g, 82%); mp 190 °C; IR (KBr) $\overline{\nu}_{max}$ (cm^{-1}): 3319, 2968, 1661 (br), 1531, 1467, 1450, 1336, 1254, 1171; ^{1}H NMR (500 MHz, $CDCl_3$) δ 7.95 (d, *J* = 7.8 Hz, 2H), 7.66 (s, 1H), 7.59 (t, *J* = 7.1 Hz, 1H), 7.47 (t, *J* = 7.6 Hz, 2H), 7.25 (t, *J* = 7.3 Hz, 3H), 7.19 (d, *J* = 7.5 Hz, 3H), 7.09 (s, 1H), 6.83 (s, 1H), 6.62 (s, 1H), 6.07 (s, 1H), 4.48 to 4.43 (m, 1H), 4.33 to 4.26 (m, 2H), 4.03 (dd, *J* = 13.4, 6.7 Hz, 1H), 3.86 to 3.82 (m, 1H), 3.37 (d, *J* = 12.9 Hz, 1H), 3.25 to 3.20 (m, 1H), 3.14 (s, 1H), 3.09 to 3.01 (m, 1H), 2.40 (s, 1H), 2.12 to 2.07 (m, 2H), 1.88 to 1.78 (m, 2H), 1.67 (s, 1H), 1.44 (s, 3H), 1.33 (s, 9H), 1.28 (s, 3H), 1.15 (t, *J* = 6.1 Hz, 6H), 0.95 to 0.98 (m, 12H); ^{13}C NMR (125 MHz, $CDCl_3$) δ 200.0, 175.2, 173.2, 172.8, 170.4, 156.6, 137.1, 136.2, 133.9, 128.9, 128.7, 128.4, 128.1, 126.9, 81.2, 58.8, 56.8, 56.4, 55.9, 53.8, 39.7, 38.7, 36.3, 35.3, 29.2, 28.2, 25.0, 23.5, 22.7, 22.5, 21.0, 19.5, 17.4; HRMS (ESI): *m/z* calcd for $C_{43}H_{65}N_6O_8$ $[M + H]^+$: 793.4864, found: 793.4868.

Boc-δOPhe-Val-Leu-Aib-Phe-Leu-Val-NH^{i}Pr (5)

Column chromatography (DCM/MeOH, 95:05); white solid (0.320 g, 60%); mp 190 °C; IR (KBr) $\overline{\nu}_{max}$ (cm^{-1}): 3361, 2978, 1641 (br), 1531, 1467, 1450, 1336, 1254, 1171; ^{1}H NMR (500 MHz, $CDCl_3$) δ 7.93 (d, *J* = 7.4 Hz, 2H), 7.74 to 7.68 (m, 1H), 7.58 (t, *J* = 7.2 Hz, 1H), 7.45 (s, 3H), 7.38 (d, *J* = 6.9 Hz, 2H), 7.28 to 7.24 (m, 3H), 7.22 to 7.14 (m, 2H), 7.12 (d, *J* = 5.6 Hz, 1H), 6.97 to 6.86 (m, 2H), 6.76 to 6.70 (m, 1H), 6.33 (s, 1H), 4.37 to 4.27 (m, 3H), 4.05 (s, 2H), 3.98 to 3.94 (m, 2H), 3.37 (d, *J* = 13.0 Hz, 1H), 3.25 (d, *J* = 7.7 Hz, 2H), 3.07 to 3.00 (m, 1H), 2.38 (s, 2H), 2.23 (d, *J* = 6.0 Hz, 2H), 1.78 (s, 4H), 1.62 (t, *J* = 7.3 Hz, 1H), 1.46 (s, 10H), 1.36 (s, 3H), 1.24 (s, 3H), 1.18 (s, 6H), 1.09 to 1.04 (m, 5H), 1.00 (d, *J* = 6.7 Hz, 2H), 0.95 to 0.87 (m, 17H); ^{13}C NMR (125 MHz, $CDCl_3$) δ 199.7, 176.4, 174.2, 173.8, 172.9, 172.5, 172.3, 170.9, 157.2, 138.0, 136.5, 133.6, 129.1, 128.7, 128.4, 128.1, 126.6, 81.1, 61.0, 59.4, 57.3, 56.8, 54.7, 53.9, 41.4, 40.0, 39.6, 36.6, 35.2, 29.7, 29.7, 28.2, 26.7, 25.4, 23.5, 23.0, 22.7, 22.4, 21.17, 19.4, 19.1, 18.1, 17.9; HRMS (ESI): *m/z* calcd for $C_{54}H_{85}N_8O_{10}$ $[M + H]^+$: 1005.6389, found: 1005.6397.

Boc-εOPhe-Val-Aib-Leu-Val-NH^{i}Pr (6)

Column chromatography (petroleum ether/EtOAc, 20:80); white solid (0.300 g, 80%); mp 220 °C; IR (KBr) $\overline{\nu}_{max}$ (cm^{-1}): 3312, 2964, 1662 (br), 1531, 1467, 1450, 1336, 1254, 1171; ^{1}H NMR (500 MHz, $CDCl_3$): δ 7.95 (d, *J* = 7.5 Hz, 2H), 7.65 (s, 1H), 7.60 (t, *J* = 7.4 Hz, 1H), 7.48 (t, *J* = 7.7 Hz, 2H), 7.25 (d, *J* = 6.6 Hz, 1H), 7.18 (d, *J* = 5.5 Hz, 1H), 6.78 (d, *J* = 7.7 Hz, 1H), 6.72 (s, 1H), 5.89 (s, 1H), 4.54 to 4.43 (m, 1H), 4.18 to 4.14 (m, 1H), 4.08 to 4.04 (m, 1H), 3.91 (s, 1H), 3.86 (s, 1H), 3.09 (t, *J* = 6.0 Hz, 2H), 2.48 (s, 1H), 2.17 (m, 1H), 1.90 to 1.85 (m, 2H), 1.75 (s br, 4H), 1.56 (s, 3H), 1.50 (s, 10H), 1.44 (s, 3H), 1.18 (d, *J* = 6.5 Hz, 3H), 1.14 (d, *J* = 6.6 Hz, 3H), 0.99 (d, *J* = 6.9 Hz, 6H), 0.96 (d, *J* = 6.6 Hz, 6H), 0.93 (d, *J* = 6.9 Hz, 3H), 0.89 (d, *J* = 5.8 Hz, 3H);^{13}C NMR (125 MHz, $CDCl_3$): δ 200.0, 175.6, 174.2, 173.67, 171.1, 170.9, 137.1, 133.5, 128.8, 128.1, 81.3, 61.1, 58.9, 57.2, 56.9, 54.1, 41.3, 40.1, 37.4, 30.4, 29.6, 29.1, 28.3, 27.4, 25.3, 23.4, 22.6, 22.2, 20.8, 19.8, 19.5, 18.8, 18.5, 17.6; HRMS (ESI): *m/z* calcd for $C_{40}H_{67}N_6O_8$ $[M + H]^+$: 759.5020, found: 759.5022.

4.4 | X-ray diffraction

Single crystals of the peptides were grown by slow evaporation from solutions in methanol-water, acetonitrile-water, or methanol-dichloromethane. Crystallization of peptide **4** yielded two polymorphic forms (**4a** and **4b**) in the triclinic space group *P*1 with different unit cell parameters. **4a** and **6** crystallized with two independent peptide molecules in the asymmetric unit, while **1**, **4a**, **4b**, and **5** have cocrystallized solvent molecules in their asymmetric units. X-ray diffraction data were collected at 293 K on a Bruker SMART APEX CCD diffractometer (Billerica, Massachusetts) using graphite monochromated MoKα radiation (λ = 0.71073 Å). Data were acquired using a combination of ϕ and ω scans. The structures were solved by direct methods using SHELXS[24] (peptides **3**, **4b**, and **6**) or SHELXD[25] (peptides **1**, **2**, **4a**, and **5**) and were refined against F^2 with full-matrix least squares method by using SHELXL-2014 program.[26] Anisotropic refinement was performed on all the nonhydrogen atoms. A partially occupied water molecule (occupancy 0.24) in **4b** was isotropically refined. Atoms C6G, C6D1, and C6D2 of the Leu6 side chain in **5** showed positional disorder, which was refined with an occupancy ratio 0.63:0.37. Hydrogen atoms of the water molecule in **1** and the amide hydrogen atom bonded to N1 in peptide **2** were located from the electron density maps and were refined isotropically. All the other hydrogen atoms were geometrically fixed and were refined as riding over the atoms to which they are bonded. The details of crystallization

and structure refinement are provided in Table S2. CCDC 1853324 (**1**), 1853325 (**2**), 1561916 (**3**), 1853326 (**4a**), 1853327 (**4b**), 1853328 (**5**), and 1561917 (**6**) contain the supplementary crystallographic data for this paper. These data are provided free of charge by The Cambridge Crystallographic Data Centre (www.ccdc.cam.ac.uk).

ACKNOWLEDGEMENTS

MK and Archana thank UGC India for senior research fellowships. We thank Science and Engineering Research Board, Department of Science and Technology India, for funding this work through the grant SB/S5/GC-07/2014.

ORCID

Ramesh Ramapanicker https://orcid.org/0000-0002-7717-6843

REFERENCES

1. Ghadiri MR, Granja JR, Buehler LK. Artificial transmembrane ion channels from self-assembling peptide nanotubes. *Nature*. 1994;369(6478):301-304.
2. Zhang S, Holmes T, Lockshin C, Rich A. Spontaneous assembly of a self-complementary oligopeptide to form a stable macroscopic membrane. *Proc Natl Acad Sci U S A*. 1993;90(8):3334-3338.
3. Zhang S, Holmes TC, DiPersio CM, Hynes RO, Su X, Rich A. Self-complementary oligopeptide matrices support mammalian cell attachment. *Biomaterials*. 1995;16(18):1385-1393.
4. Holmes TC, Lacalle S, Su X, Liu G, Rich A, Zhang S. Extensive neurite outgrowth and active synapse formation on self-assembling peptide scaffolds. *Natl Acad Sci USA*. 2000;97(12):6728-6733.
5. Aggeli A, Nyrkova IA, Bell M, et al. Hierarchical self-assembly of chiral rod-like molecules as a model for peptide β-sheet tapes, ribbons, fibrils, and fibers. *Proc Natl Acad Sci USA*. 2001;98(21):11857-11862.
6. Zhao X, Pan F, Xu H, et al. Molecular self-assembly and applications of designer peptide amphiphiles. *Chem Soc Rev*. 2010;39(9):3480-3498.
7. Matson JB, Stupp SI. Self-assembling peptide scaffolds for regenerative medicine. *Chem Commun*. 2012;48(1):26-33.
8. Hosseinkhani H, Hong PD, Yu DS. Self-assembled proteins and peptides for regenerative medicine. *Chem Rev*. 2013;113(7):4837-4861.
9. Webber MJ, Appel EA, Meijer EW, Langer R. Supramolecular biomaterials. *Nature Mater*. 2016;15(1):13-26.
10. Zhang S. Fabrication of novel biomaterials through molecular self-assembly. *Nature Biotechnol*. 2003;21(10):1171-1178.
11. Rajagopal K, Schneider JP. Self-assembling peptides and proteins for nanotechnological applications. *Curr Opin Str Biol*. 2004;14(4):480-486.
12. Gazit E. Self-assembled peptide nanostructures: the design of molecular building blocks and their technological utilization. *Chem Soc Rev*. 2007;36(8):1263-1269.
13. Burgess NC, Sharp TH, Thomas F, et al. Molecular design of self-assembling peptide-based nanotubes. *J Am Chem Soc*. 2015;137(33):10554-10562.
14. Doig AJ, MacArthur MW, Stapley BJ, Thornton JM. Structures of N-termini of helices in proteins. *M Protein Sci*. 1997;6(1):147-155.
15. Richardson JS, Richardson DC. Amino acid preferences for specific locations at the ends of alpha helices. *Science*. 1988;240(4859):1648-1652.
16. Chacko S, Ramapanicker R. Synthesis of γ-oxo γ-aryl and γ-aryl α-amino acids from aromatic aldehydes and serine. *Eur J Org Chem*. 2012;2012(36):7120-7128.
17. Marcel S, Angelika ES, Gerd D, Michael WG. Synthetic aromatic amino acids from a Negishi cross-coupling reaction. *Synthesis*. 2010;2010(2):293-303.
18. Karle IL, Balaram P. Structural characteristics of α-helical peptide molecules containing Aib residues. *Biochemistry*. 1990;29(29):6747-6756.
19. Toniolo C, Benedetti E. Structures of polypeptides from α-amino acids disubstituted at the α-carbon. *Macromolecules*. 1991;24(14):4004-4009.
20. Venkataraman J, Sankaramma SC, Balaram P. Design of folded peptides. *Chem Rev*. 2001;101(10):3131-3152.
21. Aravinda S, Shamala N, Roy RS, Balaram P. Non-protein amino acids in peptide design. *Proc Indian Acad Sci (Chem Sci)*. 2003;115(5–6):373-400.
22. Karle IL. Aspects of peptide folding and aggregation. *Acc Chem Res*. 1999;32(8):693-701.
23. Vasudev PG, Shamala N, Balaram P. Nucleation, growth, and form in crystals of peptide helices. *J Phys Chem B*. 2008;112(4):1308-1314.
24. Sheldrick GM. *SHELXS-97, a Program for Automatic Solution of Crystal Structures*. Göttingen, Germany: University of Göttingen; 1997.
25. Schneider TR, Sheldrick GM. Substructure solution with SHELXD. *Acta Crystallogr*. 2002;D58:1772-1779.
26. Sheldrick GM. Crystal structure refinement with SHELXL. *Acta Crystallogr*. 2015;C71:3-8.

SUPPORTING INFORMATION

Additional supporting information may be found online in the Supporting Information section at the end of the article.

How to cite this article: Kalita M, Archana A, Dimri A, Vasudev PG, Ramapanicker R. Synthesis of peptides containing oxo amino acids and their crystallographic analysis. *J Pep Sci*. 2019;e3148. https://doi.org/10.1002/psc.3148